

**ANALYTICAL MODELING OF THE EVOLUTION OF THE NONLINEARITY PARAMETER OF
SENSITIZED STAINLESS STEEL.**

Brian Fuchs, Jin-Yeon Kim, Laurence Jacobs
Georgia Institute of Technology
Atlanta, GA

Jianmin Qu
Tufts University
Medford, MA

ABSTRACT

Austenitic stainless steels are subject to the formation of $M_{23}C_6$ precipitates under the environmental conditions found in nuclear power generators, leaving them susceptible to corrosion due to chromium depletion at the grain boundaries. The acoustic nonlinearity parameter shows sensitivity to the formation of precipitates in 304L stainless steel. A numerical model of precipitate growth is used to show that there is a direct relationship between the predicted mean radius of $M_{23}C_6$ precipitates and the change in the acoustic nonlinearity parameter of thermally aged 304L.

Keywords: stainless steel, nonlinear ultrasound, precipitation

NOMENCLATURE

β	acoustic nonlinearity parameter
A_1	amplitude of the transmitted wave
A_2	amplitude of the second harmonic wave
I	grain boundary nucleation rate (s^{-1})
N_{GB}	grain boundary nucleation site density (m^{-3})
ω	nucleation attempt frequency (s^{-1})
G^*	activation energy barrier (J)
$S(\theta)$	precipitate shape factor
Q^*	activation energy for interface atom transfer (J/mol)
k	Boltzmann's constant ($1.38 \cdot 10^{-23} \text{ m}^2 \text{ kg K}^{-1} \text{ s}^{-2}$)
T	Temperature (K)
r	Precipitate radius (m)
V_a	Volume per atom in matrix (m^{-3})
γ_n	Matrix/nucleus interfacial energy (J/m^2)
c_i	Instantaneous concentration of solute in matrix
c_0	Starting concentration of solute in the matrix
c_∞^a	Equilibrium concentration of solute in matrix at planar interface
c^β	Concentration of solute in precipitate phase
c_r^a	Concentration of solute in matrix at interface
D	Coefficient of diffusion (m^2/s)
V_m	Molar volume of precipitate matrix (m^3/mol)
R	Universal gas constant ($8.314 \text{ J mol}^{-1} \text{ K}^{-1}$)
ϕ	Precipitate size distribution function

1. INTRODUCTION

Austenitic chromium-nickel stainless steel alloys (such as SAE 300-series) are often chosen for structural applications in the energy industry for their structural properties, creep resistance, and ability to resist corrosion even in the harsh environments seen in these applications. In nuclear energy applications, these steels are often subject to long exposure to irradiation and high temperatures. Over time, this can cause the precipitation of carbides in the steel. The dominant precipitate in 300-series steels such as 304L is $M_{23}C_6$ that forms at the grain boundaries. In a process known as sensitization, chromium in the stainless steel diffuses to grain boundaries to form these carbides, resulting in chromium-depleted zones near these boundaries. These depleted zones are susceptible to corrosive attack, including intergranular stress corrosion cracking, an insidious corrosive attack that can result in sudden catastrophic failure if not detected. [1]

Previous research in detecting microstructural damage in stainless steel has shown that nonlinear ultrasonic methods utilizing Rayleigh waves are effective in detecting precipitation in stainless steels [1,2]. When a monochromatic Rayleigh wave interacts with microscopic nonlinearities in the steel, harmonic frequencies are produced. The damage-specific ratio of the harmonic and fundamental amplitude is quantified as the acoustic nonlinearity parameter, β , with the relation:

$$\beta \propto \frac{A_2}{A_1^2 x} \quad (1)$$

A relative measure of β can be obtained by examining its change in relation to progressive damage states. There are few models in place to tie NLU results to quantitative measures of microstructural damage related to radiation.[2]

The formation of models relating carbide precipitation to nonlinear acoustic response necessitates a model of precipitate growth in stainless steel. The Kampmann and Wagner Numerical (KWN) model has been used to predict heterogeneous precipitation in aluminum [3] and steel alloys, including 300-series stainless steels.[4] This explicit model uses thermodynamic and kinetic data to predict nucleation, growth, and coarsening of precipitates. This data can be obtained from literature and from predictive thermodynamic software such as ThermoCalc.[4] The evolution of volume fraction and radius of

precipitates can then be related to the change in acoustic nonlinearity.

TABLE 1: CHEMICAL COMPOSITION OF 304L ALLOY

C	Si	Mn	Cr	Ni	Cu	S	Fe
0.019	0.55	1.66	18.37	8.13	0.39	0.026	Bal

2. MATERIALS AND METHODS

2.1 Sample Preparation

An as-received bar of wrought 304L stainless steel was cut into sections (152 mm x 50.8 mm x 15.9 mm). The 15.9 mm thickness is at least twice the Rayleigh wavelength to ensure pure Rayleigh wave generation. The alloy composition is contained in Table 1. These sections were subjected to solution heat treating (1080°C for 30 minutes, air cooled) to dissolve precipitates into the matrix. In order to induce the growth of $M_{23}C_6$ grain boundary precipitates, two samples were subjected to heat treatment at 675°C for 12 and 24 hours, followed by air cooling. Abrasive paper was then used to remove oxidation and polish the largest surfaces to 1500 grit finish.

2.2 Nonlinear Ultrasound - Rayleigh Wave Tests

Figure 1a contains a schematic of the Rayleigh wave measurement setup. An Agilent 33250A function generator was used to generate a tone burst (2.1 MHz, 30 cycles) and the signal was amplified with a RITEC GA-2500A. The amplified signal passed to an Olympus V106 contact transducer (nominal frequency 2.25 MHz). Light oil was used to couple the transducer to a wedge and a wedge to the sample. A 4 MHz Ultrasonics NCT4-D13 air-coupled transducer was used to record leaky Rayleigh waves from the surface of the sample. The signal was recorded with a Tektronix TDS 5034B oscilloscope as an average of 512 samples. Measurements were recorded at increasing incremental distance from the wedge. To process the signal, a Hann window was applied and a fast Fourier transform was used to determine magnitude of A_1 (2.1 MHz) and A_2 (4.2 MHz) (Figure 1b). β was determined using equation (1) as the slope of a linear regression of a plot of A_2/A_1^2 vs propagation distance.

2.3 Precipitation Modeling

A KWN model was used to predict the radius of $M_{23}C_6$ precipitates at the grain boundaries. A summary of the model utilized is presented in this abstract. A full outline and explanation of model parameters, initialization, and application is contained in Xiong *et al* [4].

In austenitic stainless steels, chromium is slowest-diffusing and thus the rate-controlling element for the nucleation and growth in $M_{23}C_6$. Classic nucleation theory for steady state grain boundary nucleation rate gives the equation:

$$I = N_{GB} \omega \exp \left[\frac{-G^* S(\theta) + Q^*}{kT} \right] \quad (2)$$

The radius of nucleated particles was determined by the critical radius, given by:

$$r^* = \frac{2\gamma_n V_a}{kT \ln \frac{c}{c_\infty}} \quad (3)$$

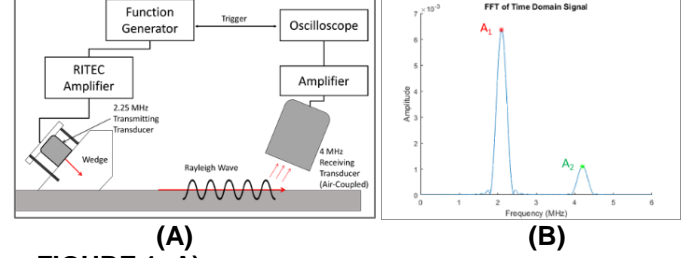


FIGURE 1: A) RAYLEIGH WAVE MEASUREMENT SETUP B) AMPLITUDE OF SOURCE AND SECOND HARMONIC WAVE

The nucleation rate is used to determine the number of particles nucleated per time step, and the particles were added to the particle size distribution with a radius of $1.1r^*$ to ensure growth in the next time step.

Growth of the particles is limited by the diffusion of Cr to the grain boundary. Precipitates were assumed to remain spherical during growth. The growth rate of each size class of precipitates is given by a collector plate model:

$$\frac{dr}{dt} = \frac{4D_{Cr,GB} \sqrt{D_{Cr,matrix}} (c_i - c_r^\alpha)}{3r^2 \sqrt{\pi} (c^\beta - c_r^\alpha)} \quad (4)$$

The concentration of solute in the matrix at the interface was determined by the Gibbs-Thomson equation for planar interfacial composition:

$$c_r^\alpha = c_\infty^\alpha \exp \left(\frac{2\gamma_n V_m}{RT} \frac{1}{r} \right) \quad (5)$$

After each time step, the new concentration of the solute in the matrix is calculated:

$$c_i = c_0 - (c^\beta - c_\infty^\alpha) \int_0^\infty \frac{4}{3} \pi r^3 \phi dr \quad (6)$$

ThermoCalc was used to determine equilibrium constants for this composition of stainless steel.

3. RESULTS AND DISCUSSION

3.1 Nonlinear Ultrasound

The Rayleigh wave measurements on the solution annealed sample provide the basis for comparison for the relative nonlinearity parameter. As aging time increased, β also increased, showing a similar trend to previous measurements [1]. The maximum β measured was at 24 hours, showing an increase of approximately 25%.

3.2 Precipitation Modeling

Table 2 contains the equilibrium volume fraction of phases in 304L stainless steel at 675°C. The σ -phase is the dominant precipitate at equilibrium. However, previous studies of 300-series stainless steels indicate that $M_{23}C_6$ growth dominates at early stages of precipitation, [4,5] so it is assumed that σ -phase does not contribute to the change in the nonlinearity parameter here.

TABLE 2: EQUILIBRIUM VOLUME PERCENTAGE OF PHASES IN 304L STEEL AT 675°C

σ	$M_{23}C_6$	MnS	γ -Fe
7.7	0.34	< 0.1	Bal

The mean precipitate radius and change in nonlinearity parameter are plotted in Figure 2. The mean radius of $M_{23}C_6$

precipitates increases to 10 nm at 24 hours, mirroring the increase in the nonlinearity parameter. This indicates a direct relationship between the growth of the $M_{23}C_6$ grain boundary precipitates and the increase in β . Further investigation into the nature of this relationship is required.

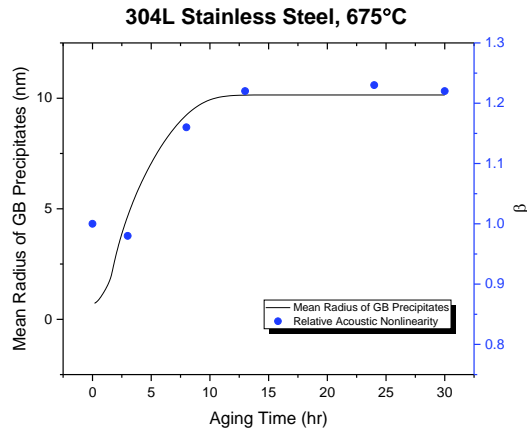


FIGURE 2: EVOLUTION OF GRAIN BOUNDARY PRECIPITATE RADIUS AND RELATIVE NONLINEARITY PARAMETER IN 304L STAINLESS STEEL AGED AT 675°C.

Verification of the precipitate model through quantitative analysis using scanning electron microscopy is ongoing. This will be used to better-fit the numerical model to the growth of precipitates in 300-series stainless steel.

4. CONCLUSION

The goal of this work was to predict the nonlinear acoustic response of 304L stainless steel subjected to sensitization by modeling the growth of precipitates. Comparison of the precipitation model to the relative nonlinearity parameter indicates a direct relationship between the mean radius of intergranular $M_{23}C_6$ precipitates and β . This relationship requires further analysis in order to determine a first-principles relationship between the two measurements.

ACKNOWLEDGEMENTS

This material is based upon work supported under an Integrated University Program Graduate Fellowship.

REFERENCES

[1] Doerr, Christoph, Kim, Jin-Yeon, Singh, Preet, Wall, James J., and Jacobs, Laurence J. "Evaluation of sensitization in stainless steel 304 and 304L using nonlinear Rayleigh waves." *NDT&E International*, Vol. 88, No. 1, (2017): pp. 17-23. DOI 10.1016/j.ndteint.2017.02.007. <https://www.sciencedirect.com/science/article/pii/S0963869517301160>

[2] Matlack, Katherine, Kim, Jin-Yeon, Jacobs, Laurence, and Qu, Jianmin. "Review of second harmonic generation measurement techniques for material state determination in

metals." *Journal of Nondestructive Evaluation*, Vol. 34, No. 1 (2015): pp. 1-23. DOI 10.1007/s10921-014-0273-5.

[3] Robson, Joseph, Jones, Mark, and Pragnell, Phil. "Extension of the N-model to predict competing homogeneous and heterogeneous precipitation in Al-Sc alloys." *Acta Materialia*, Vol. 51, No. 5 (2003): pp. 1453-1468. DOI 10.1016/s1359-6454(02)00540-2. <https://www.sciencedirect.com/science/article/abs/pii/S1359645402005402>

[4] Xiong, Qingrong, Robson, Joseph, Chang, Litao, Fellowes, Jonathan, and Smith, Mike. "Numerical simulation of grain boundary carbides evolution in 316H stainless steel." *Journal of Nuclear Materials*, Vol. 508, No. 1 (2018), pp. 299-309. DOI 10.1016/j.jnucmat.2018.05.074. <https://www.sciencedirect.com/science/article/pii/S0022311518301788>

[5] Vitek, J. M., and S. A. David. "The sigma phase transformation in austenitic stainless steels." *65th Annual American Welding Society Convention*, pp. 106-112 Dallas, TX, April 8-13, 1986